Proc. Natl. Acad. Sci. USA
Vol. 91, pp. 699–703, January 1994
Biochemistry

Crucial role for DNA supercoiling in Mu transposition: A kinetic study

(free energy of supercoiling/rate-determining step/activation energy)

ZHENGGAN WANG AND RASIKA M. HARSHEY

Department of Microbiology, University of Texas, Austin, TX 78712

Communicated by Franklin W. Stahl, September 20, 1993

ABSTRACT **DNA supercoiling plays an indispensable role in an early step of bacteriophage Mu transposition. This step involves formation of a nucleoprotein complex in which the Mu ends synapse and undergo two concerted single-strand cleavages. We describe a kinetic analysis of the role of supercoiling in the Mu-end synapsis reaction as measured by the cleavage assay. We observe a dependence of the reaction rate on superhelical density as well as on the length of Mu donor plasmid DNA. The reaction has a high activation enthalpy (≈67 kcal/mol). These results imply that the free energy of supercoiling is used directly to lower the activation barrier of the rate-limiting step of the reaction. Only the free energy of supercoiling associated with DNA outside the Mu ends appears to be utilized, implying that the Mu ends come together before the supercoiling energy is used. Our results suggest an essential function for the bacterial sequences attached to the ends of Mu virion DNA.**

The chemistry of the bacteriophage Mu transposition reaction involves single-strand cleavages at each Mu end (nicking), followed by joining of the nicked ends to target DNA (strand transfer) (1). Several stable intermediates in this reaction have been identified (2–4). Mu-end nicking is carried out by the transposase (A protein) and needs Mg^{2+} as well as *Escherichia coli* protein HU (ref. 5; Fig. 1). The Mu A protein exists in solution as a monomer (6) and binds to several specific sites at the left (*attL*) and right (*attR*) ends of Mu (9–11). This protein also binds to internal enhancer sites (12–14). In the presence of Mg^{2+}, a stable synaptic complex can be isolated in which the Mu ends have undergone cleavage (2, 3) and the Mu A protein has tetramerized (7). In the presence of Ca^{2+}, a precleavage synaptic complex accumulates (Fig. 1; ref. 4).

DNA supercoiling influences nearly all DNA–protein transactions by its effect on the energetics, hydrodynamic behavior, and physical structure of DNA (15–18). Supercoiling is required in the transposition step that leads to Mu-end cleavage (2). However, the superhelical density required can be reduced by the *E. coli* IHF (integration host factor) protein, which binds in the enhancer region (ref. 8; see Fig. 1). DNA supercoiling favors binding of Mu A protein to DNA (6) and has been suggested to favor the reaction of properly oriented Mu ends (19). In this study, we have used a kinetic approach to address the role of supercoiling in the step that leads to Mu-end cleavage. Our results reveal new aspects of the initial events during this reaction. They allow us to propose a model for how supercoiling accelerates the slow step in the pathway to Mu-end cleavage.

RATIONALE

According to the transition state theory (20), the difference in the free energy between substrates and transition states—

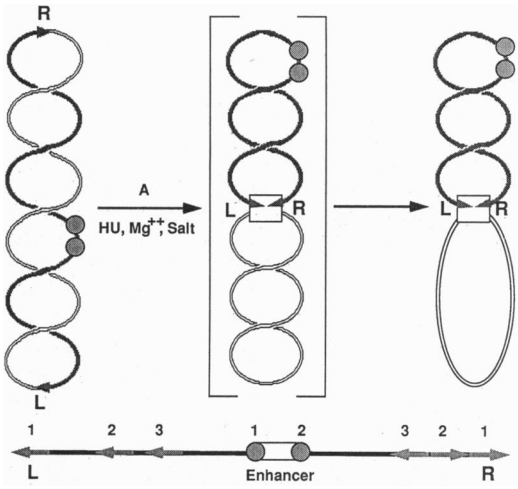

FIG. 1. The end-cleavage step of Mu transposition. Mu ends (L and R) on a negatively supercoiled plasmid (*Left*) are brought together (synapsed) and cleaved (one single-strand nick at each end) by Mu A protein to generate a stable complex. The supercoils in the Mu domain are retained, while those in the vector domain are relaxed (*Right*). A presumed intermediate has been identified in which the Mu ends have been synapsed but not nicked (*Middle*; ref. 4). The monomeric A protein (6) is found as a tetramer in the synaptic complex (7). The arrangement of A protein binding sites (three at each end and two in the enhancer) is shown below. Between the enhancer sites is a binding site for *E. coli* IHF protein. IHF stimulates the reaction when the superhelical density of DNA is low (8).

i.e., the activation energy—dictates the overall reaction rate (21):

$$k = Z\, e^{-\Delta G^{\ddagger}/RT}, \qquad [1]$$

where k is the rate constant, Z is a frequency factor, and $\Delta G^{\ddagger}$ is the free energy of activation.

Acceleration of reactions can be achieved either by reducing the energy level of the transition state, as most enzymes do, or by lifting the energy level of the substrates. In the Mu-end cleavage reaction, we propose to test whether the supercoiling energy of DNA directly contributes to reducing the free energy of activation of the rate-limiting step. Assuming that there is a single rate-limiting step in the cleavage reaction and that the supercoiling energy is used directly to lower the activation barrier, we have

$$\Delta G^{\ddagger} = \Delta G^{\ddagger 0} - \eta \Delta G_S, \qquad [2]$$

where $\Delta G^{\ddagger 0}$ is the activation free energy in the absence of supercoils and ΔG_S is the free energy of supercoiling. η is a factor we have introduced to represent the fraction of the utilizable supercoil energy.

The publication costs of this article were defrayed in part by page charge payment. This article must therefore be hereby marked "*advertisement*" in accordance with 18 U.S.C. §1734 solely to indicate this fact.

Abbreviations: IHF, integration host factor; EtdBr, ethidium bromide.

The total free energy of supercoiling in a plasmid can be approximated by

$$\Delta G_S = 10N\sigma^2RT, \quad [3]$$

where N is the number of base pairs in the plasmid, and σ is the superhelical density (22, 23). Combining Eqs. **1** and **2** with **3**, we arrive at

$$k = Z \exp\left\{ -\frac{\Delta G^{\ddagger 0} - 10\eta N\sigma^2 RT}{RT} \right\} = k_0 e^{10\eta N\sigma^2}, \quad [4]$$

where k_0 is the rate constant for the completely relaxed plasmid:

$$k_0 = Z\, e^{-\Delta G^{\ddagger 0}/RT}. \quad [5]$$

The hypothesis that the supercoiling energy could directly contribute to lowering the activation barrier of a rate-limiting step in the Mu reaction can be tested by examining the relationship between the rate constants for different topoisomers, by varying either their superhelical density or their length, as predicted by Eq. **4**. To assay the rate-limiting step directly, we must know what the product of this step is. However, in the absence of that knowledge, we can exploit the principle that the kinetics of a slow or rate-determining step will closely follow that of the overall reaction. Thus, although we measure cleavage, the kinetics should reflect that of the slow step, which we now know is formation of the uncleaved synaptic complex or Ca^{2+} complex (unpublished data; ref. 4). As kinetic resolution and methodology improve, other steps preceding the Ca^{2+} complex step could be found. Our results would be equally applicable to a preceding step, if it determines the reaction rate.

MATERIALS AND METHODS

Reagents. Mu A and *E. coli* HU proteins were purified as described (6). IHF was a gift from Howard Nash (National Institutes of Health).

Construction of Plasmids. DNA length outside the Mu ends on pRA170 (12) was manipulated to give pWZ3 (376), pWZ9 (911), pWZ14 (1460), pWZ19 (1931), and pWZ29 (2940) (the numbers 3–29 following the pWZ plasmids give the approximate DNA length outside Mu in 100-bp units, while those following in parenthesis give this exact length in bp). The Mu DNA length of this set of pWZ plasmids is 3.4 kb.

Preparation of Topoisomers. Mini-Mu plasmids were incubated with topoisomerase I in the presence of various concentrations of ethidium bromide (EtdBr), extracted with phenol, and precipitated. Superhelical density was determined by the band-counting method (24). Aliquots from different reactions were pooled to give a calibration standard with a continuous distribution of topoisomers. Samples were electrophoresed at 5°C in TPE buffer (50 mM Tris/25 mM H_3PO_4/1 mM EDTA) at ≈3 V/cm for 20 hr in the first dimension and for 15 hr in the second dimension in the presence of 1 μg of chloroquine per ml. The number of supercoils counted was converted to that under conditions of our kinetic assays after correcting for the temperature and salt dependence of the rotation angle of a DNA double helix (22, 37).

Kinetic Assay of the Nicking Reaction. Mu A, IHF, and HU proteins were added to the mini-Mu plasmids in 25 mM Tris, pH 7.5/10 mM $MgCl_2$/130 mM NaCl at 30°C. Reactions were stopped with either 20 mM EDTA or 0.2% SDS (final). The final concentration of DNA, A, HU, and IHF was, respectively, 36 μg/ml, 67 μg/ml, 10 μg/ml, and 0.2 μg/ml. This mixture was electrophoresed in the presence of 1 μg chloroquine per ml at ≈3 V/cm for 40 hr at 5°C (1.2% agarose gel). Gels were stained in EtdBr at 1 μg/ml overnight, destained in 1 mM $MgSO_4$ for 1–2 hr, and photographed with Polaroid film type 55 or 665.

Data Analysis. Negative films were scanned with a BioImage system (Millipore); DNA bands were quantitated by the whole band analysis routine. Some films were digitized in the laboratory of P. Serwer (University of Texas Health Science Center, San Antonio) as described (25) and analyzed with the National Institutes of Health IMAGE 1.41 software.

RESULTS

Kinetics of the Mu-End Cleavage Reaction. To see whether the rate constant varied with the superhelical density in a manner predicted by Eq. **4**, we first examined the kinetics of the Mu-end nicking reaction (see Fig. 1), using pRA170 DNA having a range of superhelical densities (Fig. 2 *Left*). The topoisomers with higher superhelical densities were better substrates. To analyze the kinetics of reaction of each topoisomer, the DNA bands were quantified (see *Materials and Methods*). Assay conditions were optimized (see the legend to Fig. 2 *Left*) in expectation of exponential decay kinetics. Indeed, the disappearance kinetics of the DNA substrates fit an integrated first-order equation (Fig. 2 *Center*). The rate constants were obtained from the best-fitting parameters and were plotted against the superhelical density (Fig. 2 *Right*). Assuming that the supercoiling energy contributes directly to reducing the activation barrier, we fitted the derived rate constants with Eq. **4** (Fig. 2 *Right*, solid line). Using N = 7300 bp, the total length of pRA170, we obtained a value for $\eta \approx 0.065$, which suggests that the efficiency of utilization of supercoil free energy for the whole plasmid is rather low.

Although the absolute value of the rate constants varied from experiment to experiment for individual topoisomers, their relative ratios were highly reproducible. From the best-fitting parameters of Eq. **4** (Fig. 2 *Right*), the rate constant for the completely relaxed form of pRA170 was calculated as $k_0 = 1.4 \pm 0.5 \times 10^{-5}$ s^{-1}, which corresponds to a half-time ($t_{1/2}$) of about 5×10^4 s or ≈14 hr at 30°C. In other words, under these assay conditions, the reaction of relaxed DNA substrates is too slow to generate significant product before the A protein loses activity ($t_{1/2}$ of free Mu A protein is ≈15–20 min at 30°C).

Dependence of the Reaction Rate on the DNA Length Outside Mu Ends. To test whether the dependence of the reaction rate on DNA length also follows Eq. **4**, we constructed a series of mini-Mu plasmids with different DNA lengths both inside and outside the Mu ends and determined their reaction rate. The DNA length inside was varied from 1.1 kb to 4.9 kb, inclusive of the Mu ends. Preliminary kinetic assays showed no obvious differences in the reactivity of plasmids varying in length inside the Mu domain, whereas striking differences were seen in the rate of reaction of plasmids with differing lengths outside the Mu domain (data not shown). The reaction kinetics of the latter plasmids (pZW3–pZW29; see *Materials and Methods*) were therefore examined further.

Fig. 3 *Left* shows the kinetic assay, performed as before, except that the reaction was stopped by addition of 20 mM EDTA so that the cleaved synaptic complexes (C) could be resolved from any nicked (N) and unreacted supercoiled (S) substrates. To eliminate possible systematic errors in the comparison of reaction rates, all except the smallest plasmid pZW3 (monitored on a separate gel) were mixed in the same tube before the reaction. It was difficult to resolve all bands on an agarose gel when pZW3 was included. Furthermore, the reaction of pZW3 was too slow to be quantified at the superhelical densities appropriate for other plasmids. The disadvantage of mixing all of the plasmids was that the individual topoisomers could not be resolved for determination of these rate constants. The reaction rate is therefore an average of all topoisomers for each plasmid family. Exami-

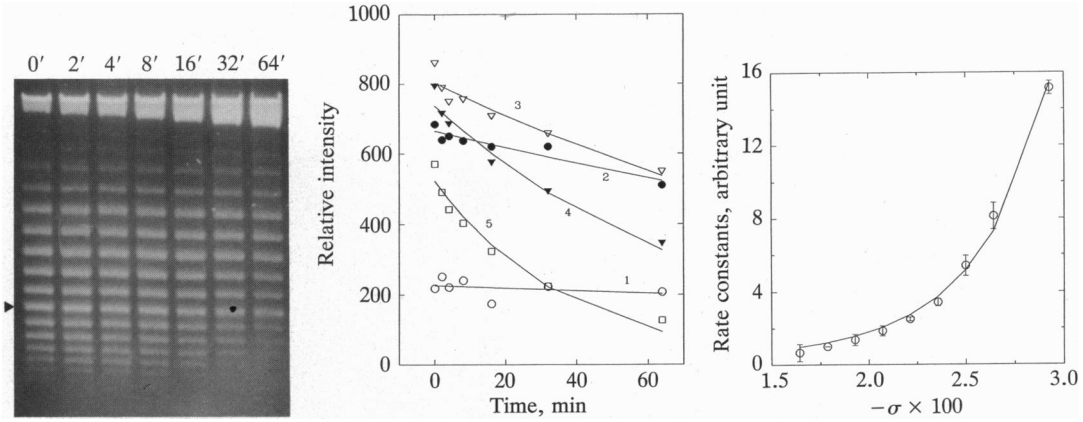

FIG. 2. Kinetics of the cleavage reaction. (*Left*) Topoisomers of mini-Mu plasmid pRA170 were assayed for Mu-end cleavage by monitoring the disappearance of the substrates at the indicated time in minutes. The concentration of A protein was in large molar excess over the DNA substrate. Concentration of accessory factors HU and IHF was optimized such that doubling their concentration did not result in a significant change in the reaction rate. The arrowhead indicates a topoisomer with a linking number deficit of −19.5. The topoisomer bands vary in steps of one, with increasing linking deficit from top to bottom. (*Center*) The DNA bands from the gel in *Left* were scanned and quantified. The time course of disappearance of the topoisomers was fitted with an integrated first-order equation ($S = S_0 e^{-kt}$, solid lines). Curves 1–5 indicate topoisomers with the following increasing superhelical densities: −0.0179, −0.0207, −0.0236, −0.0264, and −0.0293. The rate constants were obtained from the best-fitting parameters. (*Right*) Rate constants (obtained as described in *Center*) were plotted against plasmid superhelical density σ. Data points are an average of three experiments. The error bar indicates the standard error of the mean. The solid line is a two-parameter fit to Eq. **4**.

nation of the gel shows that the plasmids with more DNA outside Mu ends (larger numbers) are better substrates. To have the same reaction rate, the shorter plasmids must have a higher superhelical density. These data are shown in Fig. 3 *Center*, where the percentage of cleaved synaptic complexes [C/(C+S); C and S refer to cleaved complexes and supercoiled substrates, respectively] formed with each plasmid is plotted against the average superhelical density. From this graph, we obtained the midpoints for formation of the synaptic complexes.

In Fig. 3 *Right*, the superhelical density at which 50% cleaved complexes were formed is plotted against the total length (in bp) of each plasmid. To see how this result compares with the hypothesis that the free energy of supercoiling is used to lower the activation barrier, we rearrange Eq. **4**:

$$N = \frac{1}{10\eta\sigma^2} \ln \frac{k}{k_0}. \qquad [6]$$

Assuming that the rate constant for completely relaxed DNA is the same for all plasmids irrespective of length (k_0 = 1.4×10^{-5} s^{-1} as calculated for pRA170), we tried to fit the

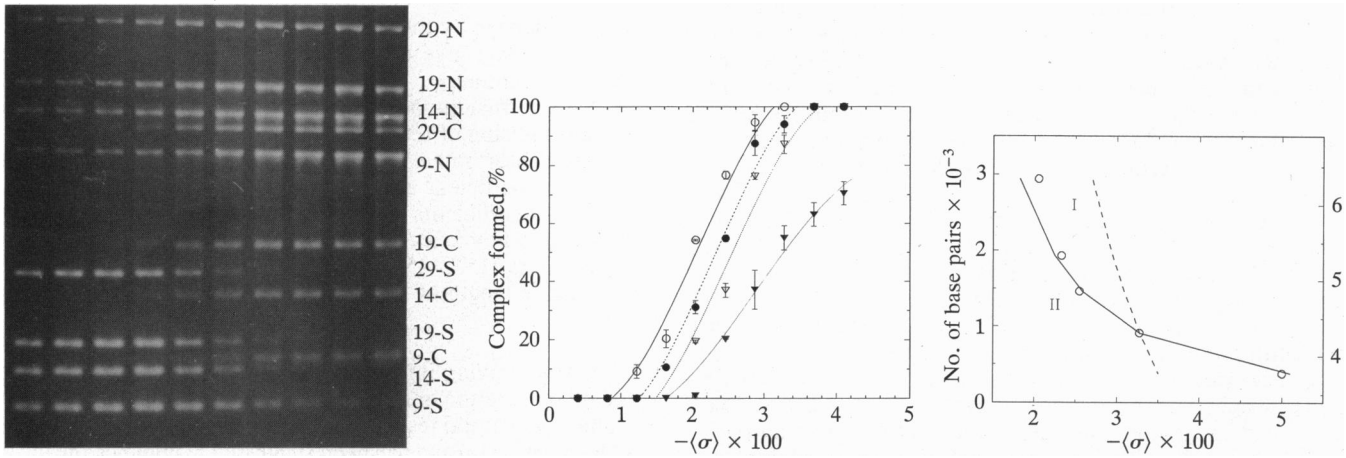

FIG. 3. Dependence of the reaction rate on the distance outside Mu ends. (*Left*) Plasmids with various outside lengths were mixed together and treated with topoisomerase I to generate different superhelical densities that increase from left to right as follows: −0.0041, −0.0082, −0.0123, −0.0164, −0.0205, −0.0246, −0.0287, −0.0328, −0.0369, −0.041. Mu-end cleavage reaction conditions were similar to those described in Fig. 2, except that the reaction was stopped with 20 mM EDTA after a 30-min incubation at 30°C and electrophoresed in the presence of EtdBr at 1 μg/ml. The numbers on the right indicate the approximate distance in bp × 100 between the two Mu ends. N, C, and S refer to nicked plasmids (relaxed), synaptic complexes (supercoiled in Mu domain, relaxed in vector domain), and supercoiled substrates, respectively. (*Center*) The DNA bands shown in *Left* were quantified, and the percentage of the cleaved synaptic complex [C/(C+S)] formed with each plasmid was plotted against the average superhelical density of each mixture. ○, pWZ29; ●, pWZ19; ▽, pWZ14; ▼, pWZ9. Drawn through the data points for each plasmid is a cubic spline function from which the following midpoints (σ at which 50% synaptic complex was formed) were obtained: −0.0327, −0.0255, −0.0233, and −0.0205 for pWZ9, pWZ14, pWZ19, and pWZ29, respectively. (*Right*) The superhelical density at which 50% synaptic complex was formed was plotted either against the total length (right scale) of the plasmid DNA or the length outside Mu. The value for pWZ3 was an estimated average from two experiments. The broken line is a one-parameter fit, with N being the total length of each plasmid. The solid line is similar to the broken one, but with N being the outside length only, and divides the quadrant into two regions. Points in region I indicate an efficiency of energy utilization (η) of <33%, while region II represents an efficiency of >33%.

data with Eq. 6. (We have used an average rate constant $\langle k \rangle$ for k, and an average superhelical density $\langle \sigma \rangle$ for σ, in the fitting. $\langle k \rangle$ was computed from the apparent $t_{1/2}$ of reaction for each plasmid population, using the equation $\langle k \rangle = \ln 2 / t_{1/2\ \text{apparent}}$.* Failure of the fit is obvious when the total length of the plasmid is used (Fig. 3 *Right*, broken line). This may imply either that our hypothesis is incorrect or that we have used the wrong parameters. Indeed, three lines of evidence suggest that only supercoiling energy associated with the DNA outside Mu is utilized. First, in the overall cleavage reaction (Fig. 1), supercoils inside the Mu domain appear unchanged at the end of the reaction (8). Second, as stated above, variation in the length of the non-Mu domain, but not the Mu domain, yielded obvious differences in the reaction rates. Third, the fitness of our model is reasonably good only when the distance outside the Mu ends is used (Fig. 3 *Right*, solid line). Although none of these three observations, when considered alone, provide convincing evidence that only the supercoiling energy associated with DNA in the non-Mu domain is used, taken together they strongly argue the case.

When only the DNA length in the non-Mu domain is used to fit the data (Fig. 3 *Right*, solid line), we obtained $\eta \approx 0.33$. Thus η, the efficiency of utilization of supercoil energy, has a much higher value when only the supercoils outside the Mu ends are seen contributing to the reaction.

We can now reestimate the value of η from the derived rate constants in the kinetic experiments shown in Fig. 2. Using $N = 2300$ (the DNA length outside Mu ends in pRA170) instead of the total length of 7300 bp, we calculate $\eta \approx 0.21$. This compares well with the value computed from the set of plasmids in the experiments described above ($\eta \approx 0.33$). We note that the apparent value of η was lower (for reasons unknown) for plasmids with DNA length longer than 1.9 kb in the non-Mu domain (Fig. 3 *Right*), consistent with the fact that η for pRA170 (2.3 kb in the non-Mu domain) was slightly lower. The good agreement between the two values of η computed from two independent sets of experiments supports our hypothesis that the free energy of supercoiling contributes to the increased rate of the reaction.

It could be argued that changing the DNA length might change steric factors that are rate-determining. We note that the reaction kinetics of the smallest plasmid pZW3 showed no significant difference when 5 bp were inserted into the DNA outside the Mu ends on this plasmid (data not shown). Since steric factors would impact the proper alignment of reactive DNA sites, insertion of 5 bp would have changed this alignment and thus affected the reaction rate, suggesting that steric factors are not likely to be rate determining in this case. This result (i.e., that the length effect is not due to steric reasons but rather due to a requirement for the free energy of supercoiling) also supports the assumption made above that, at least within a limited range, relaxed DNA substrates have a reaction rate that is independent of their length.

Temperature Dependence of the Cleavage Reaction. To gain more insight into the nature of the cleavage reaction, we examined the temperature dependence of the reaction rate. Fig. 4 shows the reaction kinetics at different temperatures (from 15°C to 35°C). As before, the kinetic data were fitted with an integrated first-order equation to obtain the rate constants for individual topoisomers at all temperatures examined. Because of the temperature dependence of the rotation angle of a DNA double helix (22), the topoisomers which comigrate in the different lanes across the agarose gel do not have the same superhelical density when assayed at different temperatures used in the transposition assays. To make a meaningful comparison, therefore, the computed rate constants were interpolated as described below.

*In this experiment, $\langle k \rangle$ is a constant, and $\langle \sigma \rangle$ is the variable for the different plasmids. We varied $\langle \sigma \rangle$ to see at what superhelical density an apparent $t_{1/2}$ of 30 min could be reached for the plasmid population.

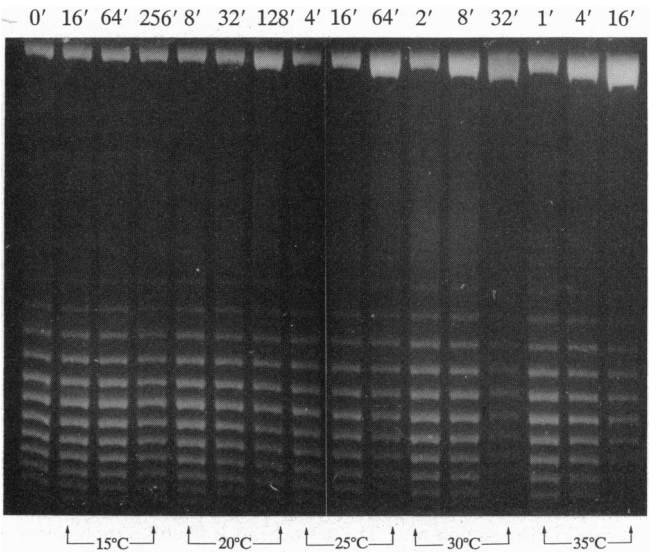

FIG. 4. Temperature dependence of the cleavage reaction. Reaction conditions were as described in the legend to Fig. 2 except that incubation temperature varied from 15°C to 35°C. Time is shown in min.

Since the dependence of the nicking rate on superhelicity could be modeled well by Eq. 4 in the range of superhelical densities shown in Fig. 2 *Right*, we used that equation to fit the rate constants obtained at various temperatures. From the difference in the reaction rates of the fitted curves at different temperatures, we calculate the average activation enthalpy to be 67 ± 15 kcal/mol using the following equation:

$$k = Z \exp\{-\Delta G^{\ddagger}/RT\}$$

$$= Z \exp\{-\Delta H^{\ddagger}/RT\} \exp\{\Delta S^{\ddagger}/R\}. \quad [7]$$

As evidenced by the rather large standard deviation of the mean, the data give us only an approximate value for the activation enthalpy. The high activation enthalpy argues against a diffusion-controlled rate-limiting step, an example being a collision of reactive sites on DNA. For such events, the encounter rates will be a function of the segmental diffusion coefficient and persistence length (17). Generally, diffusion coefficients have a low temperature dependence (less than a few kcal/mol). In the temperature range of our experiments (15°C–35°C), there is little dependence of the persistence length of DNA on temperature (26).

DISCUSSION

DNA supercoiling influences the replication, transcription, and recombination of DNA (27, 28). Supercoiling is known to promote structural features in DNA favorable for interaction with proteins (16) and has been suggested to enhance the local concentration of DNA sites that react with proteins (29). In this study we have investigated whether and in what manner DNA supercoiling influences the nicking reaction of Mu transposition. We have shown that the rate of the overall reaction depends on plasmid superhelical density and on the length of DNA outside the Mu ends, results that can be well accounted for by a model in which the free energy of supercoiling directly lowers the activation barrier of the rate-limiting step of the reaction.

The reaction shows a strong temperature dependence in the temperature range of 15°C–35°C. A rather high activation enthalpy (67 ± 15 kcal/mol) for the reaction was calculated from these experiments, suggesting that the rate-limiting

event is an energetically costly one. Such events could include structural transitions in DNA (see ref. 18). If, for example, the transition state involves DNA melting, and if the average enthalpy change of melting a base pair is 8 kcal/mol (30), then the activation enthalpy of 67 kcal/mol would indicate that melting of about 8 bp (more, if the region is A+T-rich) is involved in the transition state. Structural transitions in DNA could facilitate single-strand cleavages by the A protein. Energetically costly events could also include large conformational changes in the A protein to activate it for Mu-end cleavage. [We note that supercoils (not linking number) can be lost, and supercoiling energy can be utilized (converted) without breaking the DNA backbone. Familiar examples include conversion of supercoiling energy into tighter binding of EtdBr and conversion from positively to negatively supercoiled DNA by changing temperature.]

If supercoiling energy is indeed used in the manner suggested above, the factor η used in our kinetic analysis may indicate how well this energy is coupled to the conformational change in DNA or protein. We have implicitly assumed that η is constant at all superhelical densities (Figs. 2 *Right* and 3 *Right*). This may not be true, however. In fact, the reaction rate levels off as the supercoils are gradually increased. This may indicate either that η is a function of superhelicity and decreases with increasing superhelical density or that some other step becomes rate-limiting when the rate of the step requiring supercoiling is greatly increased. The close fit of our model to the data and the agreement between the two values of η computed from two independent sets of experiments favor the second possibility.

The free energy released by unwinding a supercoiled DNA was shown to be independent of DNA length and dependent only on superhelical density for a small change (relative to the total number) of supercoils (31). If the change in number of supercoils is comparable to the number of existing supercoils, as is likely for the Mu reaction (in Fig. 3 *Center* at 50% complex formation, the number of supercoils τ in the non-Mu domain would be $N\sigma/10.5$, which is $\approx$1.9 for pZW3, $\approx$2.9 for pWZ9, etc.), then the length of the DNA and therefore the total number of supercoils at a given superhelical density will have a significant effect on the reaction rate. As pointed out by Courey and Wang (32), under most conditions used to study structural transitions of DNA, the kinetic barrier may be so high that such transitions can take place only at high superhelical densities (33, 34). The free energy required to complete such transitions is only a fraction of the total free energy available. However, if structural transitions can occur at low superhelicity with assistance from proteins so that the cost of these transitions becomes comparable to the stored free energy of supercoiling, then the total free energy of supercoiling decides the equilibrium of the transitions. Under such circumstances, the length of the DNA and its superhelical density, which determine total free energy, become critical factors.

Our results allow us to distinguish several steps in the nicking reaction. First, the Mu ends come together to allow domain closure—i.e., division of the DNA into separate Mu and non-Mu domains. Next, the supercoiling energy is used selectively from the non-Mu domain to promote a rate-limiting step. Recent experiments suggest that this step is most likely the formation of the uncleaved intermediate (Fig. 1) and that the supercoils are not needed for the subsequent cleavage step, which is fast (unpublished data; ref. 4). The Mu enhancer, which is also required for synaptic complex formation but not for nicking (14), may function in domain closure or in formation of the complex, or both.

Our results lead us to propose an essential function for the bacterial DNA covalently attached to both ends of Mu virion DNA (35). These sequences (50–150 bp at the left end and 500–3000 bp at the right end) are acquired as a result of headful packaging of Mu DNA integrated into the bacterial genome. Upon entry into *E. coli*, infecting Mu DNA can be recovered as a circular, supercoiled DNA–protein complex in which the heterogeneous bacterial ends are noncovalently joined by the help of a protein (36). These bacterial sequences would form the outside domain when the Mu ends synapse. We suggest that the supercoiling energy in this domain serves to drive the integration of Mu into the host chromosome.

We thank Howard Nash for IHF, and Steve Levene, Paul Hagerman, Tom Kodadek, and Makkuni Jayaram for helpful comments on this work, which was supported by the National Institutes of Health (GM 33247).

1. Mizuuchi, K. (1992) *Annu. Rev. Biochem.* **61,** 1011–1051.
2. Craigie, R. & Mizuuchi, K. (1987) *Cell* **51,** 493–501.
3. Surette, M. G., Buch, S. J. & Chaconas, G. (1987) *Cell* **49,** 253–262.
4. Mizuuchi, M., Baker, T. A. & Mizuuchi, K. (1992) *Cell* **70,** 303–311.
5. Craigie, R., Arndt-Jovin, D. J. & Mizuuchi, K. (1985) *Proc. Natl. Acad. Sci. USA* **82,** 7570–7574.
6. Kuo, C. F., Zou, A., Jayaram, M., Getzoff, E. & Harshey, R. M. (1991) *EMBO J.* **10,** 1585–1591.
7. Lavoie, B. D., Chan, B. S., Allison, R. G. & Chaconas, G. (1991) *EMBO J.* **10,** 3051–3059.
8. Surette, M. G. & Chaconas, G. (1989) *J. Biol. Chem.* **264,** 3028–3034.
9. Nakayama, C., Teplow, D. B. & Harshey, R. M. (1987) *Proc. Natl. Acad. Sci. USA* **84,** 1809–1813.
10. Craigie, R., Mizuuchi, M. & Mizuuchi, K. (1984) *Cell* **39,** 387–394.
11. Zou, A., Leung, P. C. & Harshey, R. M. (1991) *J. Biol. Chem.* **266,** 20476–20482.
12. Leung, P. C., Teplow, D. B. & Harshey, R. M. (1989) *Nature (London)* **338,** 656–658.
13. Mizuuchi, M. & Mizuuchi, K. (1989) *Cell* **58,** 399–408.
14. Surette, M. G. & Chaconas, G. (1992) *Cell* **68,** 1101–1108.
15. Benham, C. J. (1985) *Annu. Rev. Biophys. Biophys. Chem.* **14,** 23–45.
16. Zechiedrich, E. L. & Osheroff, N. (1990) *EMBO J.* **9,** 4555–4562.
17. Hagerman, P. J. (1988) *Annu. Rev. Biophys. Biophys. Chem.* **17,** 265–286.
18. Wang, J. C. (1984) *J. Cell Sci. Suppl.* **1,** 21–29.
19. Craigie, R. & Mizuuchi, K. (1986) *Cell* **45,** 793–800.
20. Eyring, H. (1935) *Chem. Rev.* **17,** 65–77.
21. De Vault, D. (1984) *Quantum-Mechanical Tunnelling in Biological Systems* (Cambridge Univ. Press, Cambridge, U.K.).
22. Depew, R. E. & Wang, J. C. (1975) *Proc. Natl. Acad. Sci. USA* **72,** 4275–4279.
23. Pulleyblank, D. E., Shure, M., Tang, D., Vinograd, J. & Vosberg, H.-P. (1975) *Proc. Natl. Acad. Sci. USA* **72,** 4280–4284.
24. Shure, M. & Vinograd, J. (1976) *Cell* **8,** 215–226.
25. Griess, G. A., Moreno, E. T. & Serwer, P. (1992) in *Methods in Molecular Biology*, eds. Burmeister, M. & Ulanobsky, L. (Humana, Totowa, NJ), Vol. 12, pp. 173–181.
26. Hagerman, P. J. (1981) *Biopolymers* **20,** 1503–1535.
27. Wasserman, S. A. & Cozzarelli, N. R. (1986) *Science* **232,** 951–960.
28. Wang, J. C. & Giaever, G. N. (1988) *Science* **240,** 300–304.
29. Vologodskii, A. V., Levene, S. D., Klenin, K. V., Frank-Kamanetskii, M. & Cozzarelli, N. R. (1992) *J. Mol. Biol.* **227,** 1224–1243.
30. Cantor, C. R. & Schimmel, P. R., eds. (1980) *Biophysical Chemistry* (Freeman, San Francisco), Vol. 3.
31. Davidson, N. (1972) *J. Mol. Biol.* **66,** 307–309.
32. Courey, A. J. & Wang, J. C. (1983) *Cell* **33,** 817–829.
33. Peck, L. J., Nordheim, A., Rich, A. & Wang, J. C. (1982) *Proc. Natl. Acad. Sci. USA* **79,** 4560–4564.
34. Shimizu, M., Hanvey, J. C. & Wells, R. D. (1989) *J. Biol. Chem.* **264,** 5944–5949.
35. Harshey, R. M. (1988) in *The Bacteriophages*, ed. Calendar, R. (Plenum, New York), Vol. 1, pp. 193–224.
36. Harshey, R. M. & Bukhari, A. I. (1983) *J. Mol. Biol.* **167,** 427–441.
37. Bauer, W. R. (1978) *Annu. Rev. Biophys. Bioeng.* **7,** 287–313.